

Effect of grain refinement on enhancing critical current density and upper critical field in undoped MgB₂ ex situ tapes

A. Malagoli, V. Braccini, M. Tropeano, M. Vignolo, C. Bernini et al.

Citation: *J. Appl. Phys.* **104**, 103908 (2008); doi: 10.1063/1.3021468

View online: <http://dx.doi.org/10.1063/1.3021468>

View Table of Contents: <http://jap.aip.org/resource/1/JAPIAU/v104/i10>

Published by the [American Institute of Physics](#).

Related Articles

Development of 10 kA high temperature superconducting power cable for railway systems

J. Appl. Phys. **111**, 063910 (2012)

Enhancement of superconducting properties in FeSe wires using a quenching technique

J. Appl. Phys. **111**, 013912 (2012)

High transport critical current densities in textured Fe-sheathed Sr_{1-x}K_xFe₂As₂+Sn superconducting tapes

Appl. Phys. Lett. **99**, 242506 (2011)

Low noise measurement system for determination of the critical currents in superconducting tapes by a pulse method

Rev. Sci. Instrum. **82**, 114701 (2011)

Microstructure dependence of the c-axis critical current density in second-generation YBCO tapes

J. Appl. Phys. **110**, 083923 (2011)

Additional information on J. Appl. Phys.

Journal Homepage: <http://jap.aip.org/>

Journal Information: http://jap.aip.org/about/about_the_journal

Top downloads: http://jap.aip.org/features/most_downloaded

Information for Authors: <http://jap.aip.org/authors>

ADVERTISEMENT



**FIND THE NEEDLE IN THE
HIRING HAYSTACK**

Post jobs and reach
thousands of hard-to-find
scientists with specific skills



<http://careers.physicstoday.org/post.cfm> **physicstoday** JOBS

Effect of grain refinement on enhancing critical current density and upper critical field in undoped MgB₂ *ex situ* tapes

A. Malagoli,^{1,a)} V. Braccini,¹ M. Tropeano,¹ M. Vignolo,¹ C. Bernini,¹ C. Fanciulli,¹ G. Romano,¹ M. Putti,¹ C. Ferdeghini,¹ E. Mossang,² A. Polyanskii,³ and D. C. Larbalestier³

¹CNR-INFM LAMIA, Corso Perrone 24, I-16152 Genova, Italy

²Grenoble High Magnetic Field Laboratory, CNRS, 25 Avenue des Martyrs, B.P. 166, 38 042 Grenoble Cedex 9, France

³National High Magnetic Field Laboratory, Florida State University, Tallahassee, Florida 32310, USA

(Received 25 July 2008; accepted 4 October 2008; published online 18 November 2008)

Ex situ powder-in-tube MgB₂ tapes prepared with ball-milled, undoped powders showed a strong enhancement of the irreversibility field H^* , the upper critical field H_{c2} , and the critical current density $J_c(H)$ together with the suppression of the anisotropy of all of these quantities. J_c reached 10^4 A/cm² at 4.2 K and 10 T, with an irreversibility field of about 14 T at 4.2 K, and H_{c2} of 9 T at 25 K, high values for not-doped MgB₂. The enhanced J_c and H^* values are associated with significant grain refinement produced by milling of the MgB₂ powder, which enhances grain boundary pinning, even if at the same time also reducing the connectivity from about 12% to 8%. Although enhanced pinning and diminished connectivity are in opposition, the overall influence of ball milling on J_c is positive because the increased density of grains with a size comparable with the mean free path produces strong electron scattering that substantially increases H_{c2} , especially H_{c2} perpendicular to the Mg and B planes. © 2008 American Institute of Physics.

[DOI: [10.1063/1.3021468](https://doi.org/10.1063/1.3021468)]

I. INTRODUCTION

It is now widely believed that magnesium diboride (MgB₂) is a potential alternative to the Nb-based superconductors due to its lower raw material costs, its possibility for cryocooler use at around 20 K, and its reasonable upper critical field (H_{c2}) values. These advantages would be strengthened by further raising the irreversibility field H^* , which corresponds approximately to H_{c2}^\perp because of the strong effect that H^* has on the whole $J_c(H, T)$ curve. The highest H_{c2} values were obtained on thin films, either through introducing disorder¹ or after C doping, reaching extrapolated values of 70 T in the direction parallel to the *ab* planes.² Many efforts focused on the improvement of the critical fields and the critical current density (J_c) on polycrystalline samples, wires or tapes. It has been shown how the measured J_c , that is, the practical parameter useful for applications, is a complex balance between connectivity H_{c2} and flux pinning induced by grain boundaries and precipitates.³ The highest H_{c2} values and better performances of the current-carrying capability were obtained after doping with C in different forms, i.e., C, SiC, C nanotubes or carbohydrates. Polycrystalline MgB₂ samples doped with double-wall carbon nanotubes reached extrapolated $H_{c2}(0)$ of about 44.5 T;⁴ $H_{c2}(4.2$ K) higher than 33 T and irreversibility field H^* of 29 T were obtained on *in situ* MgB₂ wires with SiC additions;⁵ a strong vortex pinning and $H_{c2}(0)$ values exceeding 40 T were attained in SiC-doped Fe-sheathed MgB₂ *in situ* tapes.³ Besides increasing H_{c2} , adding SiC to MgB₂ also significantly improves J_c of the *in situ* tapes at high fields, perhaps by

introducing a high density of structural nanodefects and nanoscale precipitates.⁶ Combining mechanical alloying on powders and C doping in *in situ* powder-in-tube (PIT) tapes allowed to reach J_c of 10^4 A/cm² at 14.3 T and 4.2 K.⁷

Often the effect of the doping in increasing the performances in magnetic field is enhanced by a simultaneous reduction in the grain size that increases the grain boundary pinning. A combination of C-substitution-induced H_{c2} enhancement as well as the strong flux pinning centers induced by grain boundaries were indicated as responsible for the high J_c - H performances (10^4 A/cm² at 4.2 K, 12 T) in MgB₂ tapes prepared by the *in situ* PIT technique by using maleic anhydride as a dopant.⁸ Grain refinement induced by high-energy ball milling C-doped powders was indicated as the reason for the increased H_{c2}^\perp and therefore H^* that reached 17.2 T at 4.2 K.⁹

An alternative way of introducing pinning centers and increasing H_{c2} is neutron irradiation. In an experiment performed on polycrystalline samples H_{c2} exceeded 30 T (Ref. 10) while at the same time grain boundaries, pointlike defects, and local variations of the superconducting order parameter contributed to the strong pinning.¹¹ This method, though scientifically interesting, cannot be applied practically to tapes and wires.

Most of the data reported in the literature in terms of enhanced H_{c2} and J_c has been performed on *in situ* samples. However, the *ex situ* process is of great practical importance too. Recently Herrmann *et al.*⁷ reported high J_c values also for undoped *in situ* tapes, i.e., 10^4 A/cm² at 12.1 T and 4.2 K. Very good results have been recently achieved on *ex situ* samples: we performed ball milling with and without C on *ex situ* PIT tapes,¹² and reported better J_c values of 10^4 A/cm²

^{a)}Electronic mail: andrea.malagoli@lamia.infm.it.

at 4.2 K and 13 T for the C-doped sample. Senkowicz *et al.*⁹ analyzed the effect of ball milling and at the same time of C doping on H_{c2} and J_c in *ex situ* bulk samples, attaining 10^4 A/cm² at 14 T. From a performance viewpoint, there thus seems to be no decisive difference between *in situ* and *ex situ* MgB₂.

In this paper we analyze the behavior of *ex situ* PIT tapes prepared with undoped ball-milled MgB₂ powders and report a strong enhancement of both H_{c2} and $J_c(H)$, together with the suppression of the anisotropy of both these quantities. We ascribe such results to strong grain refinement and enhanced grain boundary density, which has the doubly positive effect of enhancing grain boundary vortex pinning and enhancing the electron scattering, which increases H_{c2} . Our results are thus very important from an applications point of view since ball milling can be easily applied to production quantities of MgB₂ powders, and the *ex situ* PIT method has been already demonstrated on industrial lengths.¹³

II. EXPERIMENTAL DETAILS

MgB₂ powders were prepared from commercial amorphous B (95%–97% purity) and Mg (99% purity): the powders were mixed and underwent a heat treatment at 900 °C in Ar. High-energy ball milling was conducted in a planetary ball mill with tungsten carbide (WC) jar and media for different times up to 256 h.

Monofilamentary tapes were fabricated following the *ex situ* conventional PIT method.¹⁴ MgB₂ powders were packed inside Ni or Fe tubes, which were groove rolled and drawn down to a diameter of 2 mm, then cold rolled in several steps to tapes of about 0.35 mm in thickness and 4 mm in width. The superconducting transverse cross section of the conductor was about 0.2 mm². The conductors were then subjected to a heat treatment at a temperature between 900 and 950 °C for 18 min in flowing argon atmosphere. During the final heat treatment a Ni_{2.5}MgB₂ reaction layer forms between the Ni sheath and the MgB₂ core,¹⁵ and such a layer does not allow the Ni sheath to be peeled off. Although Fe-sheathed tapes also produce a tiny reaction layer between Fe and B, it is easy to mechanically remove the sheath.⁶ Microstructural analysis and resistive measurements of the MgB₂ core itself therefore became possible by using a removable Fe sheath, avoiding any undesirable effect or superimposed signal due to the magnetic sheath.

The microstructure of MgB₂ was investigated using scanning electron microscopy (SEM) to evaluate the particle size, and x-ray diffraction (XRD) was performed in order to identify the phase, give an estimation of its orientation, and calculate the grain size.

Magneto-optical imaging was employed to assess the local nature of current flow.^{16,17} 3–5 mm long tapes were placed on the cooling finger of a continuous flow optical cryostat located on the X-Y stage of a polarized optical microscope in reflective mode. The Bi-doped garnet indicator film with in-plane magnetization was placed directly on the bare core of the MgB₂ tapes to register the normal component of magnetic flux at the tape surface.^{16,17}

Short pieces of about 6 mm in length cut from the Ni-

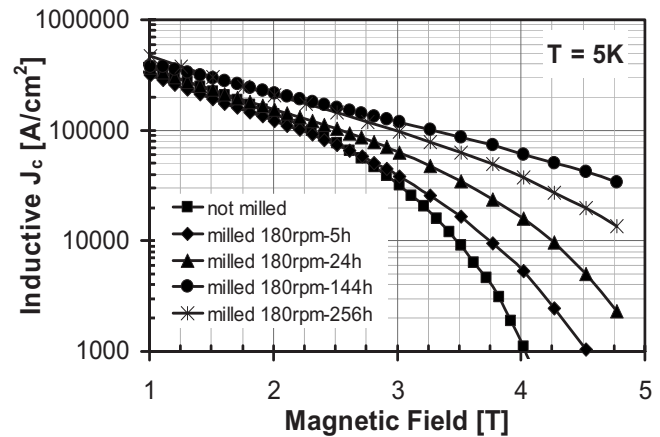


FIG. 1. Magnetic J_c vs magnetic field at 5 K in perpendicular orientation for tapes fabricated with MgB₂ powders milled for different times. J_c was evaluated from SQUID magnetization measurements and are thus lower than conventional transport.

sheathed tapes were employed for the magnetization measurements in a 5.5 T Magnetic Properties Measurement System (MPMS) Quantum Design superconducting quantum interference device (SQUID) magnetometer. The magnetic field was applied perpendicular to the tape surface and critical current density values were extracted from the M - H loops applying the Bean model. Demagnetization corrections are negligible at fields above 0.7 T, that is, the saturation field of Ni.¹⁸

Transport critical current (I_c) measurements were performed over ~ 10 cm long samples at the Grenoble High Magnetic Field Laboratory (GHMFL) at 4.2 K in magnetic field up to 13 T, applied both perpendicular and parallel to the tape surface, while the current was applied perpendicular to the magnetic field. The criterion for the I_c definition was $1 \mu\text{V}/\text{cm}$.

Resistive H_{c2} measurements were performed on the MgB₂ core of the Fe-sheathed tapes in a 9T Quantum Design Physical Properties Measurements System (PPMS) using a measuring current of 1 mA with the magnetic field applied both parallel and perpendicular to the tape surface. H_{c2} was taken to occur at 90% of the resistive transition.

III. RESULTS AND DISCUSSION

High-energy ball milling was performed on MgB₂ powders in order to lower their average grain size and improve the performance in magnetic field.¹² Figure 1 shows the critical current density J_c as a function of the magnetic field at 5 K as extracted from the M - H loops with the field perpendicular to the tape surface. We notice that even if J_c is not affected much at lower fields, a substantial improvement is obtained in high fields by increasing the milling time up to 144 h, while upon further increasing the milling time the in-field behavior worsens.

In order to investigate the dominant pinning mechanisms, we plotted in Fig. 2 the pinning force at 5 K normalized by its maximum value as a function of the normalized magnetic field $H/H_K = H/H^* = h$. The irreversibility field was determined with a linear extrapolation of the Kramer function $F_K = J_c^{0.5} B^{0.25}$ (see inset of Fig. 2)¹² and is therefore in-

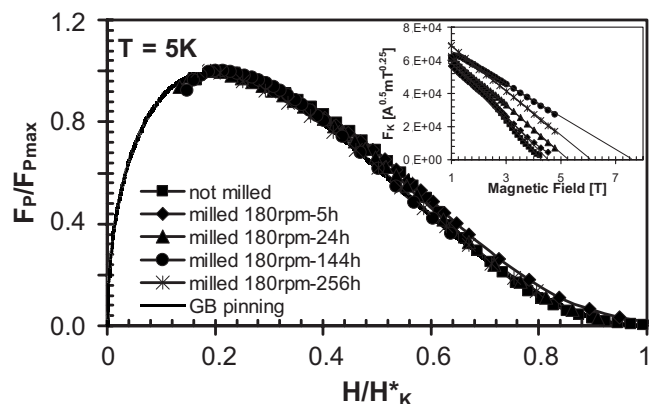


FIG. 2. Behavior of the normalized pinning force vs normalized magnetic field $h=H/H_K$ at $T=5$ K as extracted from the magnetic J_c measurements. A comparison with grain boundary pinning model $F_p=h^{0.5}(1-h)^2$ is also reported (continuous line). In the inset, the Kramer function $F_K=J_c^{0.5}B^{0.25}$ is reported as a function of the field and the linear extrapolation to estimate the irreversibility field H_K^* used to plot F_p .

indicated as the Kramer field H_K . The pinning force behavior is well described by the grain boundary pinning model $F_p=h^{0.5}(1-h)^2$ for all milling conditions. F_p rises from 3.8 GN/m^3 for the not-milled (NM) powders to 4.5 GN/m^3 for the tape prepared with powders milled for 144 h, suggesting that the ball milling process lowers the grain size and increases the number density of grain boundaries, without introducing additional pinning mechanisms on milling. The enhanced J_c in magnetic field and the higher H^* values are therefore probably due to increased perpendicular H_{c2} values, as it will be discussed later.

After investigating the ball milling parameters, we decided to focus on comparison between the tape prepared with NM powders (sample NM in the following) and the sample with the best performance in field, i.e., that prepared with powders milled for the optimum 144 h (sample M).

SEM analysis was performed on the powders. In Fig. 3 the SEM images are shown, of the powders after synthesis and milling (a), and inside the tapes after cold working and sintering (b). It is immediately clear that after milling the powders are much more homogeneous in size and smaller, and that wire fabrication produces a considerable particle refinement. We performed a statistics on about 700 particles taken from several points of the four samples in order to estimate the average diameter of the powders before and after milling and into the final tapes. The data were fitted with a Gaussian, as reported in the lower part of Fig. 3. The mean diameter values are $1.5 \mu\text{m}$ and 440 nm , respectively, for the NM and milled (M) powders, indicating a significant, even if not so strong as reported by other authors,⁹ decrease in the average diameter of the particles after milling. In the tapes, the powders are even smaller, resulting in an average diameter of 400 nm and 200 nm , respectively, in the NM and M tape.

Figure 4 compares optical and Magneto-Optical (MO) images taken on the bare core of the Ni-sheathed tapes prepared with NM (upper panel) and M (lower panel) powders. Figures 4(a) and 4(c) are the optical images of the surface of the two samples, in particular, of the Ni-sheathed tapes after removal of the sheath from both sides. Images of the fields

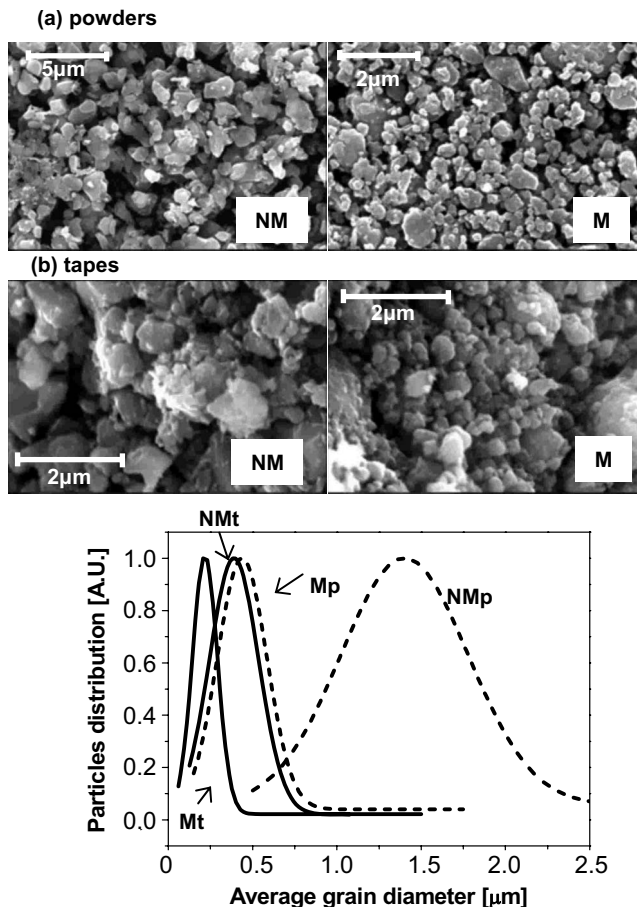


FIG. 3. SEM images of the NM and 144 h M powders (a) and NM and M tapes (b). Note that the scale bars are different. Below, the Gaussian fit of particle size distribution is reported after measuring about 500 grains for each sample. The average diameter is $1.4 \mu\text{m}$ and 440 nm for the NM and M powders (dotted lines), and 400 nm and 200 nm for the NM and M tapes, respectively.

produced by the induced currents after cooling in an external magnetic field (the Field Cooled (FC) state) of 120 mT to a temperature of 5.7 K [Fig. 4(b)] and 6.4 K [Fig. 4(d)], respectively, for the NM and M sample and then reducing the field to zero are very different. This procedure produces a trapped state throughout the whole sample, in which bright contrast areas correspond to regions of trapped magnetic flux with high J_c , while darker areas show lower J_c regions where the local trapped flux density is lower. It is clear that tape M made with M powders has a more uniform and stronger trapped flux area than the NM tape, even though the MgB_2 core size is very similar for both tapes.

In order to characterize the in-field behavior at high magnetic field, the I_c of the two samples were measured up to 13 T at GHMFL. In Fig. 5 the transport critical current I_c with field both parallel and perpendicular to the tape surface is shown. There is a remarkable increase in the critical current values in magnetic field upon milling: the J_c threshold of 10^4 A/cm^2 that is reached at 4 T in the NM sample is reached at 10 T after milling. A very striking effect is the disappearance of the J_c anisotropy after ball milling, probably due to multiple causes. The flat rolling during fabrication is likely to have a lesser texturing effect when the grains are smaller, as in the case of the M powders. Furthermore, in

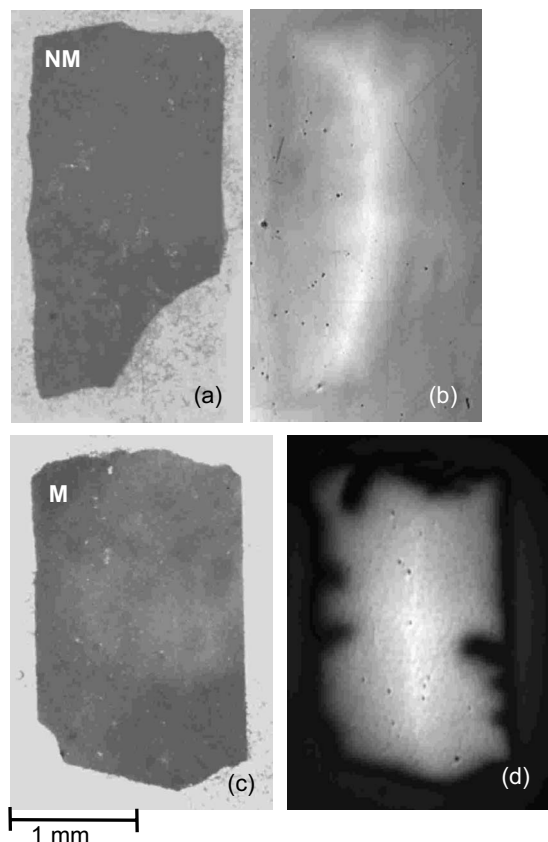


FIG. 4. Optical and MO images of the NM (upper panel) and M (lower panel) tapes after removing the Ni sheath. (a) and (c) are the optical images of the surfaces of the NM and M samples; (b) and (d) are the MO images at $H=0$ after FC in $H=120$ mT, $T=5.7$ K, and 6.4 K, respectively.

the sample with smaller grains, the meandering of the current path between adjacent grains bends more often than in the sample with larger grains, thus averaging out the relative orientation between the local current itself and the crystalline axes. Finally, ball milling introduces disorder, which is indicated by the decreased T_c (see Table I) and decreased intrinsic H_{c2} anisotropy.¹⁹

In order to be able to perform structural and superconducting property characterization of the MgB_2 core, we used the same powders to fabricate Fe-sheathed tapes from which we mechanically removed the external sheath. The magnetically evaluated J_c by dc SQUID magnetometer measurements confirmed that the superconducting behavior of the Ni- and Fe-sheathed tapes was the same.

XRD was performed on the MgB_2 cores, as reported in Fig. 6 where the results are compared with the MgB_2 starting powders. Both the powders and the cores of the tapes show a high degree of randomly oriented MgB_2 . A small amount of MgO was identified, particularly in the M powder sample. WC peaks were also detected in the M powders. The peaks have been normalized to the most intense MgB_2 peak: after milling, the peaks weaken and broaden, a sign of a decrease in the particle size.

In the inset of Fig. 6 the relative intensity of the (002) peak is shown: in the NM sample it is higher with respect to the pristine powders, showing some degree of texturing; after milling it decreases again, indicating a lower or absent tex-

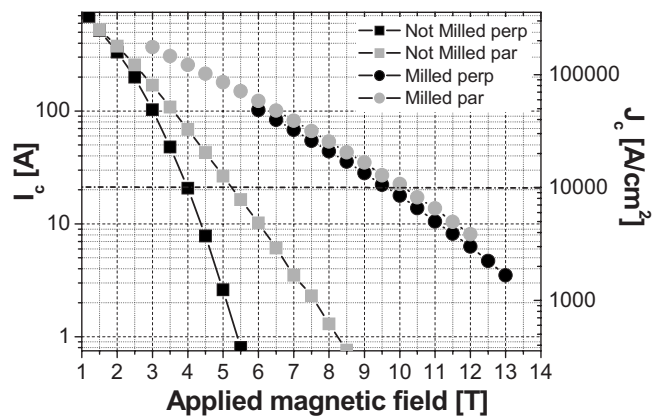


FIG. 5. Transport critical current and corresponding calculated critical current density as measured up to 13 T at GHMFL in He bath for the tapes with NM and 144 h M powders. The field was both perpendicular and parallel to the tapes' surface.

turing, consistent with the disappearance of anisotropy seen in Fig. 5 after milling. We conclude that the smaller the grains, the less effective is flat rolling in inducing texture.

The lower limit for the average crystallite size can be determined from the half width of the diffraction peaks using the Debye–Scherrer formula $D = \alpha\lambda / \beta \cos \theta$, where D is the mean particle size, α is a geometrical factor ($=0.94$), λ is the x-ray wavelength ($=1.54056$ Å), β is the half width of the diffraction peak, and θ is the angular position of the diffraction peak. By analyzing the (002) peak we obtain $D=27$ and 18 nm, respectively, for the NM and M samples, indicating a reduction in the crystallite size by ball milling. These values are much lower though than the mean particle sizes estimated by SEM analysis, indicating that the particles are polycrystalline agglomerates of much smaller crystallites.

Magnetoresistivity versus temperature was measured on the MgB_2 cores of the Fe-sheathed tapes. In Fig. 7 the resistivities are shown as a function of the temperature for the NM and M samples, and the resistive properties are summarized in Table I. In the inset of Fig. 7 the transition is magnified after the normalization of its ρ value at 40 K: the onset (90%) of the critical temperature T_c decreases after milling from 38.6 to 37 K and the transition smears, due to the disorder introduced by milling the powders. We also tried to estimate the effective current-carrying area fraction (A_F) following the Rowell analysis,²⁰ where $A_F = \Delta\rho_{\text{ideal}} / [\rho(300 \text{ K}) - \rho(40 \text{ K})]$ with $\Delta\rho_{\text{ideal}} = 7.3 \mu\Omega \text{ cm}$.²¹ The resistivity values at 40 K are quite high in both samples, 55 and 289 $\mu\Omega \text{ cm}$, respectively, a first indication of reduced connectivity in both samples. After milling, both $\rho(40 \text{ K})$ and $\rho(300 \text{ K})$ increased while at the same time the residual resistivity ratio (RRR) almost halved. The calculated effective cross-section decreased from 12% to 8%. We believe that these values provide a lower limit for the actual current-carrying fractions, and although quite low, they are comparable with many other polycrystalline samples reported in the literature where such analysis was carried out.^{3,9,22} As reported by other authors too, and also found in our case, the high resistivity values and the inferred poor connectivity do not prevent high J_c values.^{23,24} If we try to correct the measured $\rho(40 \text{ K})$ values with the effective cross section we find

TABLE I. Resistivity data and critical temperature of the tapes prepared with NM and 144 h M powders.

	$\rho(300\text{ K})$ ($\mu\Omega\text{ cm}$)	$\rho(40\text{ K})$ ($\mu\Omega\text{ cm}$)	RRR	$\Delta\rho$ ($\mu\Omega\text{ cm}$)	A_F (%)	$\rho(40\text{ K})$ corrected ($\mu\Omega\text{ cm}$)	T_c onset (K)	ΔT_c (K)
NM	116	55	2.1	61	12	6.6	38.6	0.4
M	382	289	1.32	93	8	22.7	37.0	1.6

6.6 and 22.7 $\mu\Omega\text{ cm}$, respectively, for the NM and M sample (see Table I). A linear relationship between ρ and T_c has been reported for several kinds of samples.¹⁰ With our measured critical temperature values, we expect corrected resistivity values below 10 $\mu\Omega\text{ cm}$: it is therefore likely that our samples, in particular, the M one, have an additional intrinsic source of high resistivity such as insulating phases at the grain boundaries, e.g., MgO (Ref. 25) given the fact that the controlled atmosphere has not been maintained during the whole process.²⁶ Furthermore, the inconsistency between the low current-carrying areas and the measured low-field J_c values may also be due to the fact that the current paths for the normal state and superconducting current may not be exactly the same.²⁷

In Fig. 8 the H_{c2} versus the T diagram is reported for the NM and M samples perpendicular and parallel to the tape surface. We define the 90% point of the small-current resistive transition, which itself is percolative though the weakly textured or untextured grain structure, as the parallel upper critical field H_{c2} . Besides decreasing T_c , disorder also increases H_{c2} , while at the same time suppressing its anisotropy, as well as the critical current anisotropy. The H_{c2} values reached in the M sample at 25 K are quite high, especially for undoped samples. They are comparable,^{4,28,29} or considerably higher^{8,22,30-33} than those reported for SiC or C-doped polycrystalline samples. In Fig. 9 we also report the 10% points of the resistive transitions. These provide a marker of the irreversibility line³⁰ and H_{c2} perpendicular,⁹ although occurring between H_{c2}^{\perp} and H_{c2}^{\parallel} , given that our tapes are far from being completely oriented. Figure 9 compares

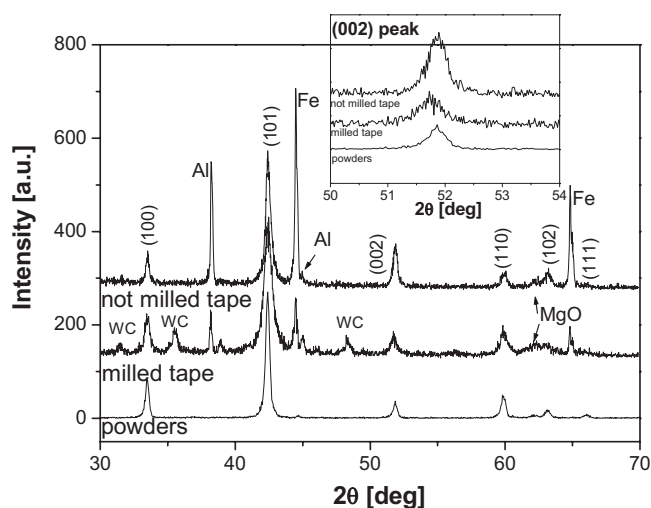


FIG. 6. XRD of MgB_2 powders compared with the core of Fe-sheathed tapes fabricated with NM and 144 h M powders. The indexed peaks come from the MgB_2 phase. In the inset, the (002) peak is magnified for the three samples.

these evaluations to a critical state evaluation of H^* (4.2 K) defined by $J_c=500\text{ A/cm}^2$, which corresponds to a critical current of 1 A flowing in the tapes. Such an estimate of H^* is clearly well below that deduced from the 10% points of the resistive transitions, even if they do show the same dependence on milling state. After milling, H^* doubled reaching about 14 T at 4.2 K, comparable with the best undoped *in situ* samples.⁷

We can now try to draw some conclusions from the competing influence of connectivity, H_{c2} and flux pinning. At all the measured magnetic fields, both from magnetic and transport measurements, the M sample has a higher J_c , consistent with its almost doubled H_{c2} . Near self-field the critical current densities are very similar, showing that milling does not degrade J_c at all, even though the connectivity of the M sample is about 1/3 lower (see Table I). There is no change in the pinning mechanisms after milling. The dominant grain boundary pinning just rises from 3.8 to 4.5 GN/m^3 due to the increased grain boundary density. J_c is in fact proportional to the inverse grain size.^{9,34} We see that particle refinement by ball milling decreases the crystallite sizes as well, increasing their number density. We think that the smaller crystallites are responsible for the raised H_{c2} by scattering electrons because the mean free path reduction enhances H_{c2} and the resistivity.¹⁰ The resistivity values corrected after calculating the effective cross-section following Rowell²⁰ (Table I) for the M sample at 40 K is 22.7 $\mu\Omega\text{ cm}$. However, as noted above this may still be an overestimate since T_c is not strongly suppressed. We believe that the real resistivity is below 10 $\mu\Omega\text{ cm}$, which would lead to a mean free path around 10 nm.¹⁰ In fact the crystallite size inferred from the XRD measurements on the M sample is around 18 nm, which is consistent with our conclusion that the crystallites act as electron scattering centers and are therefore responsible for the substantially increased H_{c2} .

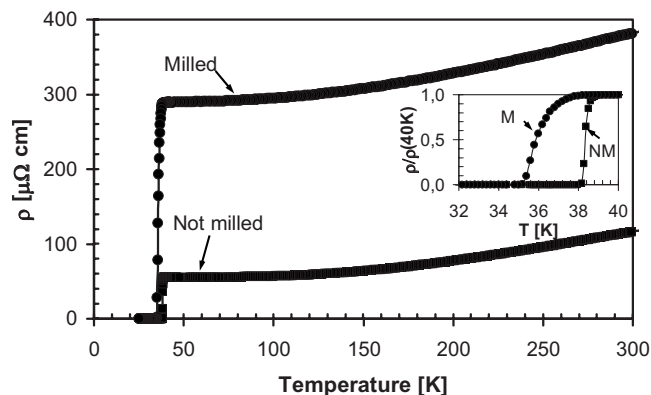


FIG. 7. Resistivity vs temperature curves of the MgB_2 tapes (after removal of the Fe sheath) prepared with NM and 144 h M powders. In the inset, the superconducting transition is magnified, normalized at 40 K.

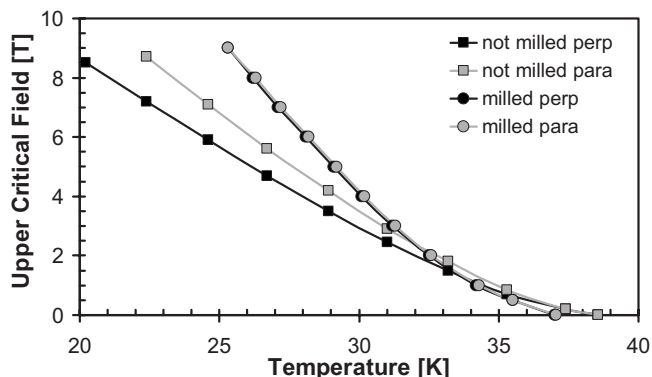


FIG. 8. H_{c2} vs T diagram (i.e., 90% of normal state resistivities from the resistive transitions in magnetic field) for the samples prepared with NM and 144 h M powders in both the perpendicular and parallel direction with respect to the tape surface. The disappearance of the anisotropy after milling is clear.

In this delicate balance between flux pinning, connectivity, and H_{c2} , we therefore think that the poor connectivity plays a lesser role while the refined crystallite size seems to be the most significant parameter responsible for enhancing J_c at high magnetic fields, as reported by several authors.^{35,36}

IV. CONCLUSIONS

In this work we studied the effect of ball milling of undoped MgB_2 precursor powders on the connectivity H_{c2} and J_c of *ex situ* PIT tapes. We optimized the milling time to obtain the best in-field performance and reached the J_c value of 10^4 A/cm² at 4.2 K and 10 T, an irreversibility field of about 14 T at 4.2 K, and H_{c2} of 9 T at 25 K, all high values for not-doped MgB_2 . The powder milling process produces a grain refinement; at the same time the calculated connectivity decreases from about 12% to 8% and the anisotropy of both the critical current and the upper critical field disappears. The increased density of grain boundaries increases the pinning force and at the same time substantially increases H_{c2} since the crystallite size is comparable with the mean free path.

The importance of such method of increasing the in-field performances of magnesium diboride lies in the fact that the

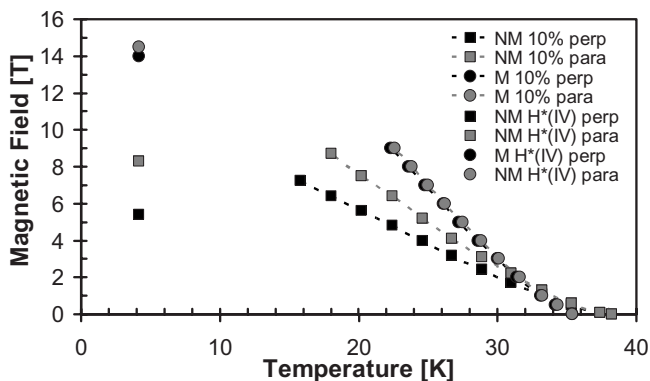


FIG. 9. 10% of normal state resistivities from the resistive transitions in magnetic field for the samples prepared with NM and 144 h M powders and measured in both perpendicular and parallel direction. At 4.2 K an estimate of the irreversibility field as the point at which the transport J_c is low enough (500 A/cm²) is reported.

milling of commercial or homemade undoped MgB_2 powders is immediately scalable to industrial quantities for the fabrication of long-length multifilamentary *ex situ* tapes with the same improved performances.

ACKNOWLEDGMENTS

Financial support by Columbus Superconductors S.p.A., by “Compagnia di S. Paolo,” by the Italian Foreign Affairs Ministry (MAE)—General Direction for the Cultural Promotion and Cooperation, by the “Transnational Access-Specific Support Action” Program Contract No. RITA-CT-2003-505474 of the European Commission, and by the EU FP6 project Contract No. NMP-3-CT2004-505724 is acknowledged. Work at Florida State University was supported by the DOE Office of High Energy Physics and the Focused Research Group on MgB_2 Contract No. DMR-0514592.

¹V. Ferrando, P. Manfrinetti, D. Marré, M. Putti, I. Sheikin, C. Tarantini, and C. Ferdeghini, *Phys. Rev. B* **68**, 094517 (2003).

²V. Braccini *et al.*, *Phys. Rev. B* **71**, 012504 (2005).

³A. Matsumoto, H. Kumakura, H. Kitaguchi, B. J. Senkowitz, M. C. Jewell, E. E. Hellstrom, Y. Zhu, P. M. Voyles, and D. C. Larbalestier, *Appl. Phys. Lett.* **89**, 132508 (2006).

⁴A. Serquis, G. Serrano, S. M. Moreno, L. Civale, B. Maiorov, F. Balakirev, and M. Jaime, *Supercond. Sci. Technol.* **20**, L12 (2007).

⁵M. D. Sumption, M. Bhatia, M. Rindfleisch, M. Tomsic, S. Soltanian, S. X. Dou, and E. W. Collings, *Appl. Phys. Lett.* **86**, 092507 (2005).

⁶Y. Zhu, A. Matsumoto, B. J. Senkowitz, H. Kumakura, H. Kitaguchi, M. C. Jewell, E. E. Hellstrom, D. C. Larbalestier, and P. M. Voyles, *J. Appl. Phys.* **102**, 013913 (2007).

⁷M. Herrmann, W. Haessler, C. Rodig, W. Gruner, B. Holzappel, and L. Schultz, *Appl. Phys. Lett.* **91**, 082507 (2007).

⁸Z. Gao, Y. Ma, X. Zhang, D. Wang, Z. Yu, H. Yang, H. Wen, and E. Mossang, *J. Appl. Phys.* **102**, 013914 (2007).

⁹B. J. Senkowitz, R. J. Mungall, Y. Zhu, J. Jiang, P. M. Voyles, E. E. Hellstrom, and D. C. Larbalestier, *Supercond. Sci. Technol.* **21**, 035009 (2008).

¹⁰C. Tarantini, H. U. Aebersold, V. Braccini, G. Celentano, C. Ferdeghini, V. Ferrando, U. Gambardella, F. Gatti, E. Lehmann, P. Manfrinetti, D. Marré, A. Palenzona, I. Pallecchi, I. Sheikin, A. S. Siri, and M. Putti, *Phys. Rev. B* **73**, 134518 (2006).

¹¹A. Martinelli, C. Tarantini, E. Lehmann, P. Manfrinetti, A. Palenzona, I. Pallecchi, M. Putti, and C. Ferdeghini, *Supercond. Sci. Technol.* **21**, 012001 (2008).

¹²V. Braccini, A. Malagoli, A. Tumino, M. Vignolo, C. Bernini, C. Fanciulli, G. Romano, M. Tropeano, A. S. Siri, and G. Grasso, *IEEE Trans. Appl. Supercond.* **17**, 2766 (2007).

¹³V. Braccini, D. Nardelli, R. Penco, and G. Grasso, *Physica C* **456**, 209 (2007).

¹⁴G. Grasso, A. Malagoli, C. Ferdeghini, S. Roncallo, V. Braccini, and A. S. Siri, *Appl. Phys. Lett.* **79**, 230 (2001).

¹⁵E. Bellingeri, A. Malagoli, M. Modica, V. Braccini, A. S. Siri, and G. Grasso, *Supercond. Sci. Technol.* **16**, 276 (2003).

¹⁶A. A. Polyanskii, D. M. Feldmann, and D. C. Larbalestier, in *Handbook of Superconducting Materials*, edited by D. Cardwell and D. Ginley (IOP, Bristol, 2003), pp. 1551–1567.

¹⁷A. Polyanskii, V. Belin, I. Felner, M. I. Tsindlekht, E. Yashchin, E. Dul’kin, E. Galystan, M. Roth, B. Senkowitz, and E. E. Hellstrom, *Supercond. Sci. Technol.* **17**, 363 (2004).

¹⁸V. Braccini, D. Nardelli, A. Malagoli, A. Tumino, C. Fanciulli, C. Bernini, A. S. Siri, and G. Grasso, *IEEE Trans. Appl. Supercond.* **15**, 3211 (2005).

¹⁹M. Putti, R. Vaglio, and J. M. Rowell, *Supercond. Sci. Technol.* **21**, 043001 (2008).

²⁰J. M. Rowell, *Supercond. Sci. Technol.* **16**, R17 (2003).

²¹J. Jiang, B. J. Senkowitz, D. C. Larbalestier, and E. E. Hellstrom, *Supercond. Sci. Technol.* **19**, L33 (2006).

²²Z. Gao, Y. Ma, X. Zhang, D. Wang, H. Yang, H. Wen, and K. Watanabe, *Appl. Phys. Lett.* **91**, 162504 (2007).

²³B. J. Senkowitz, J. E. Giencke, S. Patnaik, C. B. Eom, E. E. Hellstrom,

- and D. C. Larbalestier, *Appl. Phys. Lett.* **86**, 202502 (2005).
- ²⁴S. X. Dou, V. Braccini, S. Soltanian, R. Klie, Y. Zhu, S. Li, X. L. Wang, and D. Larbalestier, *J. Appl. Phys.* **96**, 7549 (2004).
- ²⁵M. Vignolo, G. Romano, A. Malagoli, V. Braccini, C. Bernini, M. Tropeano, A. Martinelli, V. Cubeda, A. Tumino, M. Putti, C. Ferdeghini, and A. S. Siri, *IEEE Trans. Appl. Supercond.* **18**, 1175 (2008).
- ²⁶M. Vignolo, G. Romano, A. Malagoli, V. Braccini, M. Tropeano, E. Bellingeri, C. Fanciulli, C. Bernini, V. Honkimäki, M. Putti, and C. Ferdeghini, *IEEE Trans. Appl. Supercond.* (accepted for publication).
- ²⁷H. Yamamoto, A. Tsukamoto, K. Saitoh, M. Okada, and H. Kitaguchi, *Appl. Phys. Lett.* **90**, 142516 (2007).
- ²⁸B.-H. Jun and C.-J. Kim, *Supercond. Sci. Technol.* **20**, 980 (2007).
- ²⁹B. J. Senkowicz, J. E. Giencke, S. Patnaik, C. B. Eom, E. E. Hellstrom, and D. C. Larbalestier, *Appl. Phys. Lett.* **86**, 202502 (2005).
- ³⁰H. Kumakura, H. Kitaguchi, A. Matsumoto, and H. Yamada, *Supercond. Sci. Technol.* **18**, 1042 (2005).
- ³¹Y. Ma, X. Zhang, S. Awaji, D. Wang, Z. Gao, G. Nishijima, and K. Watanabe, *Supercond. Sci. Technol.* **20**, L5 (2007).
- ³²H. Kumakura, H. Kitaguchi, A. Matsumoto, and H. Hatakayama, *Appl. Phys. Lett.* **84**, 3669 (2004).
- ³³X. Zhang, Y. Ma, Z. Gao, D. Wang, Z. Yu, and L. Wang, *Supercond. Sci. Technol.* **20**, 1198 (2007).
- ³⁴H. Kitaguchi, A. Matsumoto, H. Kumakura, T. Doi, H. Yamamoto, K. Saitoh, H. Sosiati, and S. Hata, *Appl. Phys. Lett.* **85**, 2842 (2004).
- ³⁵M. Kiuchi, H. Mihara, K. Rimura, T. Haraguchi, E. S. Otabe, T. Matsushita, A. Yamamoto, J. Shimoyama, and K. Kishio, *Physica C* **445–448**, 474 (2006).
- ³⁶M. Eisterer, *Supercond. Sci. Technol.* **20**, R47 (2007).